Journal of Geothermal Research and Volcanology (2026) 18-26

Contents lists available at FoundAE

Journal of Geothermal Research and Volcanology

Journal homepage: https://ejournal.foundae.com/index.php/jograv/index

Structural controls and radiogenic heat sources of a granite-hosted geothermal system in Belitung Island, Southeast Asia tin granite belt

Rabin Fatmansyah[a,*], Rofiqul Umam[b]

[a] Department of Physics, Institut Teknologi Sumatera, Way Huwi, Jati Agung, South Lampung, Lampung 35365, Indonesia
[b] Faculty of life and Environmental Sciences, University of Tsukuba, Tsukuba, Ibaraki 305-0006, Japan

ARTICLE INFO

Keywords:
Radiogenic geothermal system
Gravity inversion
Crustal heat production
Granite intrusion
Tin granite belt

ABSTRACT

Belitung Island forms part of the Southeast Asia Tin Granite Belt, a metallogenic province characterized by extensive granitic intrusions enriched in heat-producing elements such as thorium (Th), uranium (U), and potassium (K). The radiogenic decay of these elements generates long-lived crustal heat, providing favorable conditions for the development of non-volcanic geothermal systems. In the Bulding area of Belitung Island, surface manifestations of radiogenic hot springs suggest the presence of subsurface heat sources associated with granitic bodies. However, the geometry, depth extent, and structural controls of these potential heat sources remain poorly constrained. This study applies satellite-derived gravity data and integrated two-dimensional (2D) forward modeling and three-dimensional (3D) inversion to characterize the subsurface structure beneath Belitung Island. Free-air anomaly (FAA), elevation, and coordinate data obtained from the TOPEX dataset were processed to generate a Complete Bouguer Anomaly (CBA) map, revealing anomaly values ranging from −1.541 mGal to 55.846 mGal. The modeling results indicate the presence of high-density intrusive bodies interpreted as granite extending from depths of approximately 16.5 km to near-surface levels (~0.66 km). These bodies are inferred to represent the primary radiogenic heat source responsible for the observed geothermal manifestations. The results provide new geophysical constraints on granite-related non-volcanic geothermal systems in the Southeast Asia Tin Granite Belt and highlight the potential of gravity-based structural modeling for reducing exploration uncertainty in radiogenic geothermal provinces.

1. Introduction

Geothermal energy represents one of the most reliable and sustainable renewable energy resources available today, owing to its capability to provide continuous baseload power with minimal greenhouse gas emissions. Unlike intermittent renewable sources such as solar and wind, geothermal systems are largely independent of climatic variability and can maintain high capacity factors over extended operational lifetimes [1, 2]. For countries with rapidly growing energy demands and commitments to decarbonization, geothermal resources offer a strategic pathway toward energy security and long-term sustainability. Indonesia, located along the tectonically active margins of Southeast Asia, hosts some of the world's largest geothermal resources, predominantly associated with Quaternary volcanic arcs. Consequently, geothermal exploration and development in Indonesia have historically focused on volcanic geothermal systems characterized by high heat flow, shallow magmatic intrusions, and well-defined hydrothermal manifestations.

However, geothermal resources are not exclusively confined to active volcanic environments. Increasing attention has been directed toward non-volcanic geothermal systems, which occur in regions lacking recent magmatic activity but still exhibit measurable geothermal manifestations. These systems are often driven by alternative heat sources, including elevated regional geothermal gradients, deep crustal circulation, and radiogenic heat production within granitic intrusions [3–5]. In contrast to volcanic systems, where heat sources are typically associated with young magmatic bodies, non-volcanic geothermal systems are commonly controlled by the long-term thermal evolution of the continental crust [6, 7]. As a result, their thermal anomalies may be subtler and more structurally controlled, posing greater challenges for exploration and resource assessment [8–10].

* Corresponding author.
E-mail address: rabin.fatmansyah@gmail.com (R. Fatmansyah).

https://doi.org/10.58524/jograv.v1i1.106
Received 6 January 2026; Received in revised form 12 February 2026; Accepted 15 February 2026
Available online 5 March 2026
XXXX-XXXX/Published by FoundAE (Foundation of Advanced Education).

Among non-volcanic geothermal environments, granite-related radiogenic geothermal systems have attracted particular interest. Granitic rocks commonly contain elevated concentrations of heat-producing elements such as uranium (U), thorium (Th), and potassium (K). The radioactive decay of these elements generates sustained crustal heat over geological timescales, contributing to localized thermal anomalies even in the absence of recent magmatic intrusions [3, 11]. Regions characterized by extensive granitic provinces, especially those associated with tin-bearing belts, are therefore considered promising targets for radiogenic geothermal exploration. In such settings, the distribution, depth, and geometry of granitic bodies, as well as the presence of structural permeability pathways, play critical roles in governing hydrothermal circulation and surface geothermal manifestations [12, 13].

Belitung Island, located within the Southeast Asia Tin Granite Belt, represents one such region with significant potential for radiogenic geothermal development (Fig. 1). The Southeast Asia Tin Granite Belt extends across parts of Thailand, Malaysia, and Indonesia, and is characterized by widespread Late Paleozoic to Mesozoic granitic intrusions enriched in heat-producing elements. Belitung Island hosts numerous granitic outcrops associated with historical tin mineralization, indicating the presence of evolved, radiogenic granites [6, 14, 15]. In the Bulding area of Belitung Island, surface manifestations in the form of warm springs have been reported, suggesting the existence of a geothermal system that may be structurally and lithologically controlled by underlying granitic bodies [4, 16]. Despite these indications, the subsurface configuration of potential heat sources, the crustal architecture, and the structural controls governing geothermal circulation remain poorly constrained [17, 18].

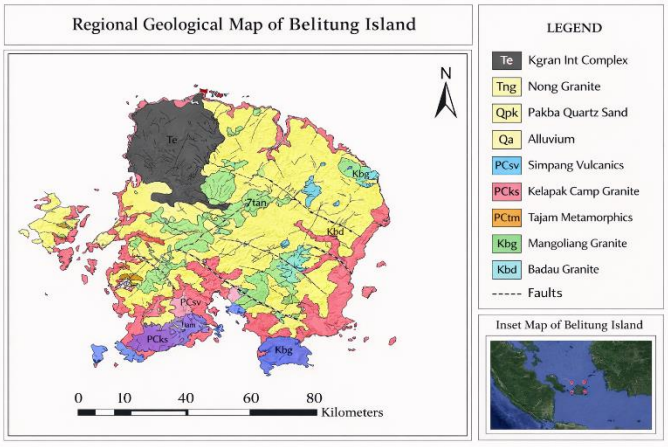

Fig. 1. Regional geological in radiogenic heat production of Belitung Island.

Understanding the crustal structure is fundamental for characterizing geothermal systems, particularly in non-volcanic settings where heat sources are not directly observable at the surface. The geometry, depth extent, and lateral continuity of granitic intrusions determine not only the distribution of radiogenic heat but also the thermal gradient within overlying sedimentary or metamorphic units [3, 6, 16]. Furthermore, fault systems and lithological contacts may act as conduits for deep fluid circulation, enabling meteoric waters to descend to depth, become heated, and ascend to the surface as geothermal manifestations. Therefore, delineating both the lithological distribution and structural framework of Belitung Island is essential for evaluating its geothermal potential [19–21].

Geophysical methods provide an effective means of investigating subsurface structures in regions where direct drilling information is limited or unavailable. Among these methods, gravity surveying is particularly useful for mapping density contrasts associated with intrusive bodies, sedimentary basins, and crystalline basement structures. Granitic rocks typically exhibit moderate to high densities compared to surrounding sedimentary units, allowing their presence to be inferred from gravity anomaly patterns. Additionally, gravity data can reveal basin geometry, basement highs, and structural lineaments that may influence geothermal fluid pathways. When integrated with two-dimensional (2D) forward modeling and three-dimensional (3D) inversion techniques, gravity analysis can provide quantitative constraints on subsurface architecture and density distribution [3, 6, 16].

Previous studies of granite-related geothermal systems have demonstrated that integrated geophysical approaches are essential for reducing exploration uncertainty. In sedimentary basin environments underlain by granitic basement, gravity data can help distinguish between deep-seated heat sources and shallow structural features. However, the inherent non-uniqueness of gravity inversion requires careful integration with geological constraints and reference density values to produce geologically plausible models. In the context of Belitung Island, where direct subsurface data are sparse, gravity-based structural characterization offers a valuable first-order assessment of geothermal potential [6, 14, 15].

Despite the recognized geothermal significance of the Southeast Asia Tin Granite Belt, comprehensive geophysical investigations focusing on radiogenic geothermal systems in Belitung Island remain limited. Most previous geothermal research in Indonesia has concentrated on volcanic provinces, leaving non-volcanic granite-hosted systems comparatively underexplored. This gap highlights the need for systematic structural characterization of granitic provinces to better understand their geothermal potential and to support diversification of Indonesia's geothermal portfolio beyond volcanic arcs [19–21].

The present study aims to characterize the crustal structure and evaluate the role of radiogenic granite bodies as potential heat sources beneath Belitung Island using gravity data analysis and integrated 2D–3D modeling. Specifically, this research seeks to: (1) delineate the spatial distribution of density contrasts associated with granitic intrusions and sedimentary units; (2) estimate the depth extent and geometry of granite bodies beneath the Bulding geothermal manifestation area; and (3) assess the structural framework that may control geothermal fluid circulation. By integrating Complete Bouguer Anomaly mapping, spectral analysis, forward modeling, and 3D inversion, this study provides quantitative constraints on the subsurface configuration of Belitung Island's granite-related geothermal system.

The outcomes of this research contribute to a better understanding of radiogenic geothermal processes within granitic provinces and demonstrate the applicability of gravity-based structural modeling for non-volcanic geothermal exploration. More broadly, the study provides a geophysical framework for evaluating geothermal potential in other segments of the Southeast Asia Tin Granite Belt and similar radiogenic provinces worldwide. Through improved characterization of crustal architecture and heat source distribution, exploration uncertainty can be reduced, supporting more informed decision-making in geothermal resource assessment and development.

2. Conceptual geological setting

2.1. *Tectonic framework of the Southeast Asia Tin Granite Belt*

Belitung Island forms part of the Southeast Asia Tin Granite Belt (SEATGB), one of the world's most extensive tin-bearing metallogenic provinces. This belt extends from mainland Southeast Asia through Peninsular Malaysia to the Indonesian islands of Bangka and Belitung. The SEATGB is characterized by widespread Late Paleozoic to Mesozoic granitic intrusions emplaced during complex tectono-magmatic events related to the convergence and accretion of continental blocks along the Sundaland margin. The tectonic evolution of the region involved

subduction, continental collision, and post-collisional magmatism, resulting in large volumes of felsic intrusive rocks enriched in incompatible and heat-producing elements [19–21].

The granites within the SEATGB are typically classified as S-type and I-type granites, many of which are highly fractionated and associated with significant tin (Sn) mineralization. Their geochemical characteristics indicate enrichment in uranium (U), thorium (Th), and potassium (K), elements responsible for long-term radiogenic heat production within the continental crust. This enrichment makes the SEATGB not only economically important for tin resources but also geothermally significant due to the potential accumulation of radiogenic heat over geological timescales.

In radiogenic granite provinces, crustal heat generation can remain elevated long after magmatic emplacement. Unlike volcanic geothermal systems driven by recent magmatic heat input, granite-related systems rely on sustained heat production through radioactive decay. Consequently, thermal anomalies in such settings are often moderate but persistent, and their geothermal viability depends strongly on crustal architecture, heat transfer mechanisms, and permeability structures.

2.2. Geological framework of Belitung Island

Belitung Island is dominated by granitic intrusions that crop out extensively across the island (Fig. 1). These granitoids are generally interpreted as part of the Late Triassic to Jurassic magmatic episode associated with the SEATGB. The granites are commonly coarse-grained, felsic, and locally mineralized, reflecting advanced magmatic differentiation processes. In addition to granitic bodies, the island comprises sedimentary and minor metamorphic units, particularly in localized basinal depressions and along structural corridors.

The basement of Belitung Island is interpreted as crystalline continental crust intruded by multiple granitic plutons. Field observations and geological mapping indicate that granite exposures are widespread, often forming topographic highs, while sedimentary deposits and Quaternary alluvium occupy lower-lying areas. These relationships suggest that the present-day surface morphology partially reflects the underlying lithological contrasts and structural controls.

From a geothermal perspective, the presence of radiogenic granite at or near the surface suggests the possibility of elevated crustal heat flow. However, surface exposure alone does not necessarily indicate an active geothermal system. The depth extent, geometry, and internal heterogeneity of the granite bodies are critical parameters controlling heat distribution. Furthermore, the presence of overlying sedimentary sequences may influence heat retention, insulation, and fluid storage capacity.

In the Bulding area of Belitung Island, reported geothermal manifestations in the form of warm springs indicate active hydrothermal circulation. These manifestations are not associated with young volcanic activity, reinforcing the interpretation that the geothermal system is non-volcanic and likely controlled by crustal radiogenic heat combined with structural permeability pathways. However, the subsurface architecture beneath this manifestation area remains insufficiently constrained, necessitating geophysical investigation [12, 13].

2.3. Granite-related radiogenic heat production

Granitic rocks are known to exhibit higher concentrations of heat-producing elements compared to mafic or ultramafic lithologies. The decay of U, Th, and K isotopes generates radiogenic heat, contributing to the overall heat budget of the continental crust. In regions where granitic bodies are voluminous and thick, cumulative radiogenic heat production can significantly elevate local geothermal gradients [12, 13].

In the context of Belitung Island, the granites of the SEATGB are likely to contribute to long-term heat accumulation within the upper and middle crust. The effectiveness of this heat source in generating a geothermal system depends on several factors:

- The thickness and lateral extent of granitic intrusions.
- The depth of emplacement and degree of exposure.
- The presence of insulating sedimentary cover.
- The development of fracture networks and fault systems facilitating fluid circulation.

Radiogenic geothermal systems are typically characterized by moderate temperatures, relatively low enthalpy compared to volcanic systems, and strong structural control. In such systems, deep meteoric water circulation along permeable faults or lithological contacts allows groundwater to descend to depth, absorb heat from the surrounding crust, and ascend to the surface. Therefore, understanding both the lithological distribution and structural framework is essential for characterizing geothermal potential [19–21].

2.4. Structural controls and crustal architecture

Belitung Island is structurally influenced by regional tectonic processes associated with the evolution of Sundaland. Fault systems and lineaments observed at regional scale may represent inherited structures reactivated during post-magmatic deformation. These structures likely play a key role in controlling fluid migration and geothermal manifestation [8–10].

In granite-dominated terrains, fractures and faults commonly develop due to cooling, tectonic stress, and exhumation processes. Such structural discontinuities enhance permeability within otherwise low-porosity crystalline rocks. Where faults intersect granite–sediment boundaries, permeability contrasts may further localize hydrothermal circulation. Consequently, the geometry of basement highs, sedimentary basins, and intrusive contacts becomes critical for understanding geothermal fluid pathways. Gravity methods are particularly well suited for delineating crustal architecture in such settings. Density contrasts between granitic intrusions and surrounding sedimentary units can produce measurable gravity anomalies, allowing the mapping of basement geometry and structural discontinuities. High-density anomalies may correspond to intrusive bodies or basement uplifts, whereas low-density anomalies may indicate sedimentary basins or fractured zones. By integrating gravity data with geological constraints, it is possible to construct a conceptual model of subsurface structure relevant to geothermal processes.

2.5. Conceptual geothermal model for Belitung Island

Based on the regional geological framework of the Southeast Asia Tin Granite Belt and the lithological characteristics of Belitung Island, a conceptual geothermal model can be proposed. In this model, granitic bodies enriched in radiogenic elements constitute the primary heat source within the crust. Heat generated through radioactive decay accumulates within the granitic mass and surrounding crustal rocks, leading to elevated geothermal gradients relative to background continental settings. Overlying sedimentary sequences, where present, may act as thermal insulators and potential reservoir units. Fault systems and fracture networks provide permeability pathways for meteoric water circulation. Groundwater infiltrates through permeable zones, descends along structural conduits, is heated at depth within or adjacent to granitic bodies, and subsequently rises to the surface, forming warm springs such as those observed in the Bulding area.

However, the viability of this conceptual model depends critically on the depth, thickness, and structural configuration of the granite bodies. If the granitic intrusions are deeply buried or laterally discontinuous, heat transfer to shallow levels may be limited. Conversely, if the granite extends to relatively shallow depths and is intersected by permeable fault systems, the conditions may be favorable for sustained hydrothermal circulation [8–10]. Therefore, constraining the crustal structure and radiogenic heat source geometry beneath Belitung Island is essential for evaluating the plausibility of this conceptual geothermal model. The integration of gravity anomaly analysis with 2D forward modeling and 3D inversion provides a quantitative framework for testing this hypothesis and refining the understanding of granite-related geothermal systems in the Southeast Asia Tin Granite Belt [12, 13].

3. Method

3.1. Study area and data source

This study was conducted between July 23 and November 25, 2022, using secondary datasets. All data processing and

interpretation were carried out in Bandar Lampung, Indonesia. The investigated area covers the entire Belitung Island and its surrounding region, located between 107°31.5′–108°18′ E and 2°31.5′–3°6.5′ S, with a total area of approximately 4,800 km².

Belitung Island lies within the Southeast Asia Tin Granite Belt and is characterized by extensive granitic intrusions and associated sedimentary and metamorphic units. The study focuses on delineating the crustal structure and identifying potential radiogenic heat sources beneath the island using gravity data analysis and integrated 2D–3D modeling.

This study utilizes publicly available satellite-derived gravity and topographic datasets, specifically Free-Air Anomaly (FAA) data and elevation data. Both datasets were obtained from the TOPEX UCSD global gravity database (http://topex.ucsd.edu). Data extraction was conducted by defining the geographic boundaries of Belitung Island and downloading the corresponding gravity and topographic data within the specified coordinate range.

In addition to the primary gravity dataset, several supporting datasets were incorporated to enhance the reliability of the analysis. These include Digital Elevation Model (DEM) data used for terrain correction, regional geological maps of Belitung Island for lithological and structural constraints, and reference rock density values compiled from published literature to guide quantitative modeling and subsurface interpretation.

The overall workflow of this study consists of five main stages. First, the geographic boundaries of the study area were defined, followed by the extraction of gravity and topographic data. Second, Bouguer anomaly calculations were performed to obtain the Complete Bouguer Anomaly (CBA) dataset. Third, spectral analysis was conducted to estimate source depths and to separate regional and residual anomaly components. Fourth, two-dimensional (2D) forward gravity modeling was carried out along selected profiles to constrain subsurface geometry and density distribution. Finally, three-dimensional (3D) inversion modeling was implemented to reconstruct the volumetric crustal structure and characterize potential radiogenic heat sources.

3.2. *Gravity data processing*

The study area boundaries were defined using Google Earth Pro. The four corner coordinates forming a rectangular boundary were determined and converted from degrees–minutes–seconds (DMS) format into decimal degrees [14, 22, 23] using equation (1).

$$Coordinate = \left[Degree(°) + \frac{Minute\ (')}{60} + \frac{Second\ ('')}{3600}\right] \quad \ldots (1)$$

These coordinates were entered into the TOPEX interface to extract elevation and FAA datasets. An optimal Bouguer density was estimated through correlation analysis between elevation and Bouguer anomaly values using density variations ranging from 1.7 to 2.3 g/cm³. The density value that minimized correlation between gravity anomaly and elevation was selected as the representative surface density. The Complete Bouguer Anomaly (CBA) was calculated as equation (2).

$$CBA = FAA - Bouguer\ Correction + Terrain\ Correction \quad \ldots (2)$$

The corrected dataset was subsequently converted into UTM Zone 48S coordinates for spatial analysis.

3.3. *Spectral analysis and regional–residual separation*

To estimate source depth and separate regional and residual components, spectral analysis was performed using Fourier Transform techniques implemented in Oasis Montaj. The logarithmic power spectrum was analyzed by plotting log amplitude against wavenumber. The slope of the spectrum was used to estimate the average depth of anomaly sources. A cut-off wavenumber was determined based on the transition between deep (regional) and shallow (residual) sources, supported by the coefficient of determination (R^2) as a control parameter. Regional and residual anomalies were separated using frequency-domain filtering:

- Low-pass filter → isolates deep regional anomalies
- Band-pass filter → highlights shallow residual anomalies

Residual anomalies are interpreted to represent shallow density contrasts related to structural features and geothermal circulation pathways.

3.4. *Two and three-dimensional forward modeling*

Two-dimensional forward modeling was conducted along selected profiles crossing significant gravity anomalies. The objective was to estimate subsurface geometry and density distribution consistent with observed gravity responses. Modeling was performed using Oasis Montaj, integrating geological constraints. A trial-and-error forward modeling approach was applied until the misfit between observed and calculated anomalies was minimized (error <5%). The minimum and maximum density values obtained from 2D modeling were used as constraints for subsequent 3D inversion modeling.

Three-dimensional gravity modeling was performed using Grablox 1.6e, with visualization in Bloxer 1.6e. The workflow consisted of:

1. Initial Forward Modeling
   A block model representing the study area was constructed based on gridded Complete Bouguer Anomaly data. Major and minor blocks were defined according to spatial resolution and area extent.
2. Density Parameter Assignment
   Density values derived from 2D modeling were assigned as initial constraints.
3. Inverse Modeling
   An iterative inversion procedure was applied to adjust density distribution and geometry to minimize misfit between observed and calculated gravity anomalies. Optimization stages included:
   - Base model adjustment
   - Density optimization
   - Occam density smoothing
   - Elevation adjustment
   - Occam height smoothing

The inversion process aimed to reduce residual error and obtain a geologically reasonable subsurface density model.

3.5. *Data interpretation*

Interpretation was conducted qualitatively and quantitatively. For the qualitative interpretation, gravity anomaly maps (Complete Bouguer, regional, and residual) were analyzed to identify patterns associated with density contrasts. High gravity anomalies were interpreted as potential granitoid intrusions or basement highs, whereas low residual anomalies were interpreted as fractured or altered zones possibly associated with geothermal fluid pathways.

While quantitative interpretation, the cross-sectional models from 2D forward modeling and volumetric density distributions from 3D inversion were integrated with geological maps. Density contrasts were correlated with lithological units and structural features, particularly fault systems that may act as geothermal conduits.

- The final interpretation focuses on identifying:
- Potential granite heat sources
- Structural controls (faults/fractures)
- Zones of reduced density indicative of hydrothermal alteration

4. Results and discussion

4.1. *Complete bouguer anomaly (CBA) map*

The complete Bouguer anomaly map (ABL) is a representation of gravity data that shows variations in rock mass density or density below the surface. The pattern of variations in rock mass density is generated from the Earth's gravitational acceleration,

which calculates differences in density relative to the mass below the surface. The results are obtained using UTM 48S coordinates with a range of anomaly values from -1.541 mGal to 55.846 mGal. The ABL map can be seen in Fig. 2.

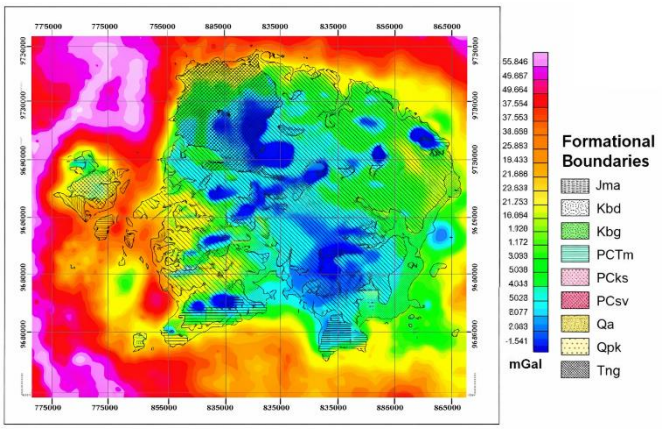

Fig. 2. Regional geological in radiogenic heat production of Belitung Island.

Gravity anomaly values are directly related to subsurface rock density, such that higher gravity anomalies generally correspond to higher-density rocks, whereas lower gravity anomalies indicate lower-density materials. In the study area, high gravity anomalies range from 25.887 mGal to 55.846 mGal, while low gravity anomalies range from −1.541 mGal to 24.323 mGal. The geothermal manifestation area is predominantly associated with low gravity anomalies. These low-anomaly zones are interpreted to reflect less compact or fractured subsurface structures characterized by relatively low density. Such structural conditions may enhance permeability, facilitating fluid circulation and allowing geothermal fluids to accumulate and emerge at the surface. Therefore, the occurrence of geothermal manifestations in the study area is interpreted to be structurally controlled by zones of reduced density and mechanical weakness within the subsurface [24].

4.2. *Spectral analysis*

Spectral analysis was applied to estimate the depth of gravity anomaly sources and to separate regional, residual, and noise components. This method is based on the Fourier transform, which converts gravity data from the spatial domain into the frequency (wavenumber) domain. In the logarithmic power spectrum, the slope of the linear segments is proportional to the depth of the causative source. Steeper gradients correspond to deeper anomaly sources (regional anomalies), whereas gentler gradients represent shallower sources (residual anomalies) [20, 21, 25].

Fig. 3 shows the Fourier transform results presented as a plot of wavenumber versus logarithmic amplitude. The spectrum exhibits three distinct linear segments, indicating three different discontinuity levels within the subsurface. The boundaries between these segments were determined based on the coefficient of determination (R^2), which was used as a control parameter to ensure the reliability of the linear fitting between the independent variable (wavenumber) and the dependent variable (log amplitude).

Based on the spectral curve, the anomaly field was divided into three zones: regional, residual, and noise components. The regional anomaly is separated by a cutoff wavenumber of 0.9712, representing deeper and broader subsurface sources. The residual anomaly is defined by a cutoff wavenumber of 0.9893, corresponding to shallower density contrasts. The noise component is identified at a cutoff wavenumber of 0.938, representing high-frequency fluctuations unrelated to geological structures.

This separation provides a quantitative basis for filtering the gravity data prior to forward and inversion modeling, thereby improving the reliability of subsurface structural interpretation.

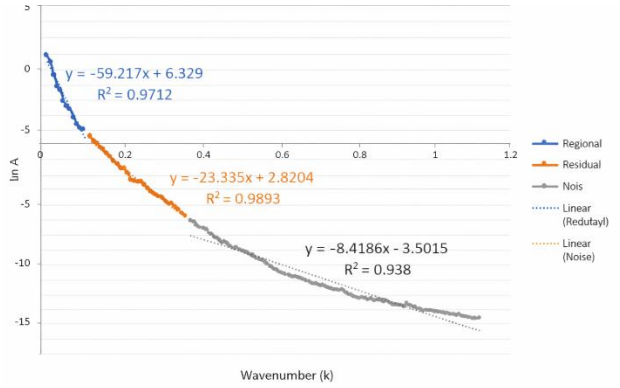

Fig. 3. Curve of spectral analysis of regional anomalies, residuals, and noise separation.

4.3. *Separation of regional and residual anomalies*

Noise-free regional and residual gravity anomaly maps were generated through filtering of the Complete Bouguer Anomaly (CBA) dataset. The separation process was performed using Butterworth and band-pass filters implemented in Oasis Montaj. The Butterworth filter was applied to distinguish between regional and residual components, while the band-pass filter was used to suppress high-frequency noise within the residual field. This filtering procedure allows the separation of deep-seated (regional) and shallow (residual) anomaly sources, thereby improving the reliability of structural interpretation.

The regional anomaly map (Fig. 4) exhibits a broader and smoother spatial distribution compared to the residual anomaly. The regional anomaly values range from −1.175 mGal to 55.973 mGal. The anomaly pattern shows relatively high values in the western part of the study area, gradually decreasing toward the central and eastern regions.

The elevated regional anomalies in the western sector are interpreted as reflecting deeper high-density basement rocks, likely associated with crystalline or granitic bodies extending beneath the surrounding offshore areas. In contrast, the central and eastern parts of Belitung Island are characterized by relatively lower regional anomaly values, which may indicate comparatively lower-density crustal materials or thicker sedimentary cover.

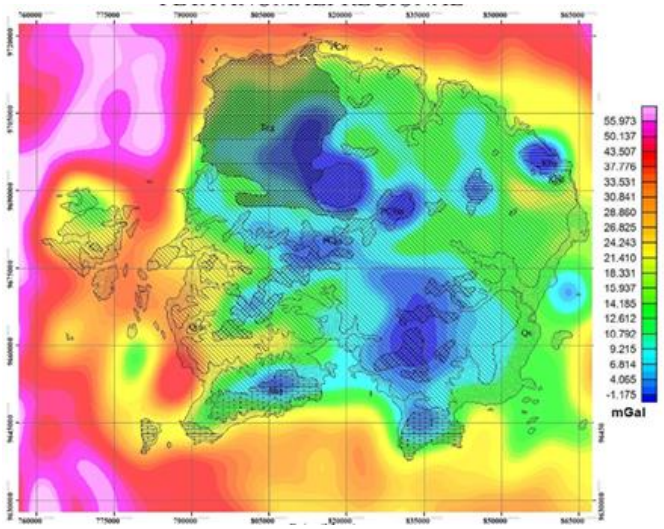

Fig. 4. Regional gravity anomaly map of Belitung Island obtained using low-pass Butterworth filtering. The map highlights long-wavelength anomaly components associated with deep-seated crustal structures. Gravity values are expressed in mGal.

The residual anomaly map (Fig. 5) was obtained by subtracting the regional component from the Complete Bouguer Anomaly dataset. The residual anomaly values range from −4.743 mGal to 3.56 mGal. Low residual anomalies occur within the range of −4.743 mGal to 0.199 mGal, whereas high residual anomalies range from 0.404 mGal to 3.56 mGal. Residual anomalies primarily reflect shallow subsurface density variations associated with local geological structures. Low residual anomalies are interpreted as zones of reduced density, possibly related to sedimentary accumulations, fractured zones, or altered rocks. Conversely, positive residual anomalies may correspond to shallow high-density bodies such as granitic intrusions or basement highs.

It is important to note that gravity values are influenced by elevation; higher topography generally corresponds to lower observed gravity due to increased distance from the Earth's center of mass, whereas lower topography tends to produce relatively higher gravity values. However, after applying Bouguer and terrain corrections, the residual anomalies predominantly reflect subsurface density contrasts rather than surface topographic effects [16, 26, 27].

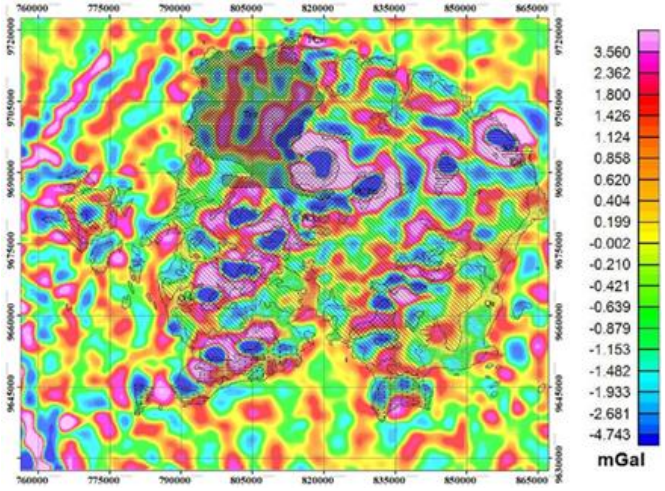

Fig. 5. Residual gravity anomaly map.

4.4. 2D gravity anomaly modeling

Two-dimensional (2D) gravity modeling was carried out using the Complete Bouguer Anomaly (CBA) map, integrated with regional geological data to constrain lithological interpretation. The selected profile lines include A–A′ (Fig. 6), which directly intersects the Bulding hot spring manifestation area. The modeling results along profile A–A′ are presented in Fig. 7. Profile A–A′ extends for more than 30 km with a maximum modeling depth of approximately 17 km. In addition, profile B–B′, which also intersects the Bulding geothermal manifestation, has a total length of approximately 58 km and a modeled depth exceeding 17 km.

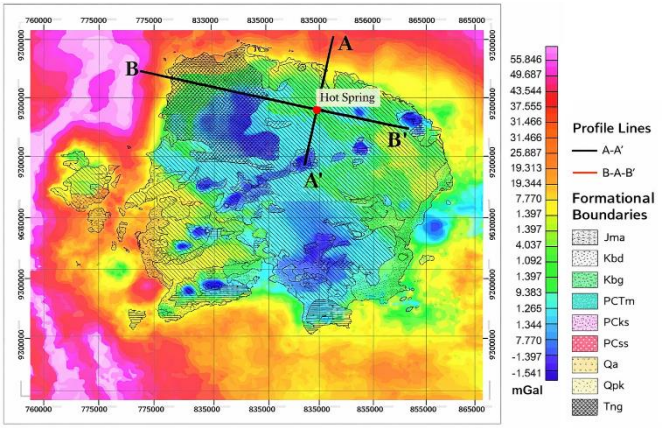

Fig. 6. Integrated geological and Complete Bouguer Anomaly (CBA) map of Belitung Island.

Both profiles reveal the presence of a fault structure cutting across the geothermal manifestation zone. This fault is interpreted as a permeable pathway facilitating fluid circulation between the subsurface heat source and the surface manifestation. The inferred heat source is associated with granitic rocks at depth, while the observed hot spring represents the surface expression of upward-migrating geothermal fluids. The structural control indicated by the intersecting fault suggests that fluid flow is strongly governed by fracture permeability within the granite-related geothermal system.

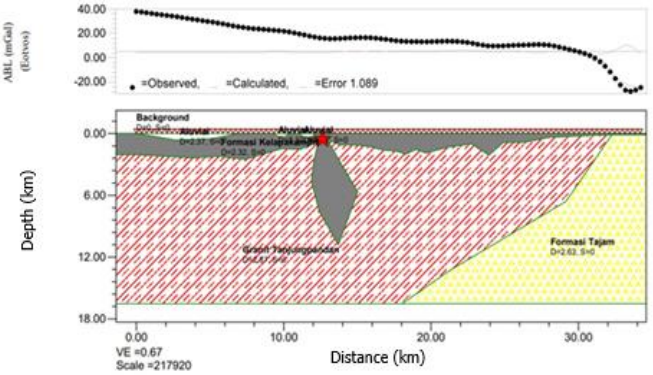

Fig. 7. Two-dimensional gravity forward model along profile A–A′ crossing the Bulding hot spring manifestation. The upper panel shows the observed and calculated Complete Bouguer Anomaly with an RMS error of 1.089 mGal. The lower panel presents the interpreted subsurface geological structure, highlighting the granite basement, sedimentary formations, and a fault zone that controls geothermal fluid circulation.

The error value obtained from the 2D modeling along profile A–A' is 1.089%, indicating a good agreement between the observed data and the modeled results. The resulting curve shows that the subsurface layers in the Building area, East Belitung, consist of four geological formations intersected by profile A–A', namely: Alluvial and Coastal Deposits (Qa), Tanjungpandan Granite (Trtg), Kelapakampit Formation (PCks), and Tajam Formation (PCTm). The Alluvial and Coastal Deposits (Qa) have a density of 2.37 g/cm³ and are composed of mixed materials such as gravel, sand, silt, clay, and coral fragments.

The Kelapakampit Formation (PCks), of Permo-Carboniferous age, has a density of 2.32 g/cm³. This formation consists of weakly to moderately folded flysch-type sedimentary rocks, composed of metamorphosed sandstone interbedded with slate, mudstone, shale, tuffaceous siltstone, and chert. The Tajam Formation (PCTm) has a density of 2.63 g/cm³ and consists of quartz-rich rocks interbedded with siltstone, exhibiting moderate to strong folding and low-grade metamorphism. The Tanjungpandan Granite (Trtg) has an average density of 2.87 g/cm³. This formation is composed of granite classified as S-type granite. The Tanjungpandan Granite is interpreted as a potential source of radiogenic heat on Belitung Island due to the presence of radioactive elements.

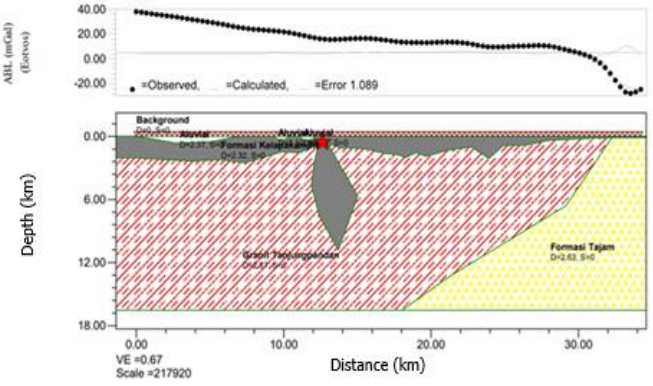

Fig. 8. Two-dimensional gravity forward model along profile B–B′ crossing the Bulding hot spring manifestation.

Along profile B–B' shown in Fig. 8, the modeling produced an error value of 3.615%, indicating a reasonable fit between the modeled results and the observed data. The modeling curve indicates that the subsurface layers along this profile consist of four geological formations: Kelapakampit Formation (PCks), Alluvial and Coastal Deposits (Qa), Tanjungpandan Granite (Trtg), and Burungmandi Granodiorite (Kbg).

The Alluvial and Coastal Deposits (Qa) have a density of 2.68 g/cm³ and are composed of mixed materials including gravel, sand, silt, clay, and coral fragments. The Kelapakampit Formation (PCks) has an average density of 2.46 g/cm³. This formation consists of weakly to moderately folded flysch-type sedimentary rocks, composed of metamorphosed sandstone interbedded with slate, mudstone, shale, tuffaceous siltstone, and chert.

The Tanjungpandan Granite (Trtg) has an average density of 2.87 g/cm³ and is classified as S-type granite. The Burungmandi Granodiorite Formation (Kbg) consists of granodiorite characterized by a light gray to greenish color, holocrystalline texture, equigranular fabric, and hypidiomorphic structure. Its mineral composition includes quartz, plagioclase, feldspar, biotite, hornblende, and secondary minerals such as chlorite, carbonate, and iron oxides. Based on geochemical analysis, this rock is classified as I-type granite.

4.5. 3D gravity anomaly modeling

The 3D modeling was conducted in two main stages: inversion modeling and forward modeling. The inversion stage aimed to achieve curve fitting between the calculated gravity response and the observed field gravity anomaly data using a mathematical modeling approach. This process was carried out to estimate unknown subsurface physical parameters, particularly rock density distribution. The initial model of the study area was constructed using a density range of 1 g/cm³ to 3 g/cm³, determined based on the previous 2D modeling results obtained from Oasis Montaj software. This initial model served as the input for the inversion process.

The inversion was performed using complete Bouguer anomaly data, followed by a series of optimization steps, including:

- Base optimization,
- Density optimization,
- Occam d optimization (density),
- Elevation optimization,
- Occam h optimization (height).

These optimization steps were conducted to minimize the error value by refining the estimation of subsurface physical parameters. The Occam h optimization (height) was applied to optimize the elevation distribution of each model block, thereby improving the agreement between observed and calculated gravity data [16].

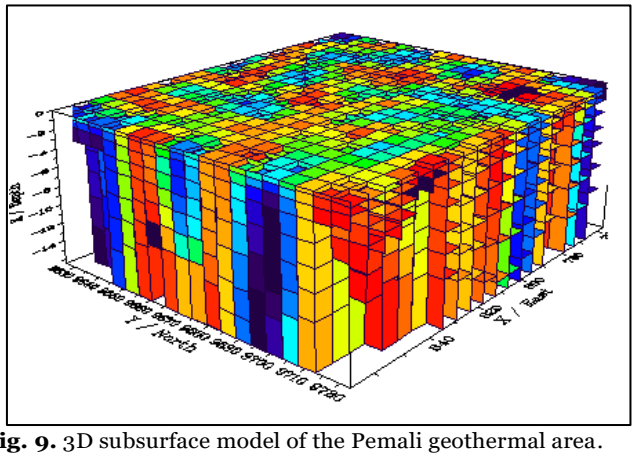

Fig. 9. 3D subsurface model of the Pemali geothermal area.

The results of the Occam h optimization indicate that high gravity anomalies are concentrated in the western part of the study area, while low anomalies dominate the central part of Belitung Island. The final Occam h result represents the integration of all optimization stages and provides the best-fit Bouguer anomaly pattern between the calculated model and the measured data (Fig. 9).

After completing both inversion and forward modeling, the 3D subsurface model was visualized using Bloxer 1.6e software. The 3D modeling results for Belitung Island are shown in Figure 9, displaying four different viewing perspectives. The 3D model reveals subsurface structures down to a depth of approximately 16.5 km, divided into eight layers. The density variation within the model ranges from 1 g/cm³ to 3 g/cm³. Density contrasts in each block are represented using a color scale, illustrating the spatial distribution of subsurface rock density variations [16].

Fig. 10 presents the fifth layer model at depths ranging from approximately 4 km to 6 km, with density values varying between 1 g/cm³ and 2.99 g/cm³. The 3D modeling results indicate the presence of an intrusive granitic body penetrating the overlying rock units. This granitic body is interpreted as part of the Tanjungpandan Granite Formation, characterized by high-density values (represented in red). In contrast, lower-density zones (represented in blue) are interpreted as rocks belonging to the Kelapakampit Formation, including sandstone units that form part of its lithological composition.

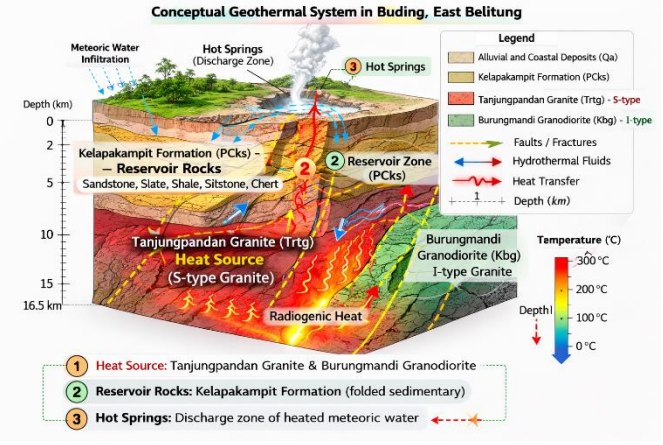

Fig. 10. Integrated conceptual geothermal model of the Buding system, East Belitung, illustrating intrusion-related heat generation and structurally controlled hydrothermal circulation. Deep granitic bodies act as radiogenic heat sources, while folded sedimentary formations serve as permeable reservoirs. Faults and fractures facilitate upward heat transfer and meteoric fluid convection, resulting in hot spring manifestations at the surface.

Further interpretation based on the 2D models along profiles A–A' and B–B' indicates that the geothermal system in the Buding area is composed of the Kelapakampit Formation, Alluvial Deposits, and Tanjungpandan Granite. Each formation exhibits distinct density characteristics. The Kelapakampit Formation, forming the basal layer, has an average density ranging from 2.32 g/cm³ to 2.46 g/cm³, extending to depths of approximately 6.39 km along both profiles. Meanwhile, the Tanjungpandan Granite exhibits average density values between 2.68 g/cm³ and 2.87 g/cm³, reaching depths of up to 16.5 km. In the Buding geothermal system, the Kelapakampit Formation is interpreted to function as a reservoir, as its sedimentary rocks allow the accumulation and circulation of meteoric water infiltrating into the subsurface. In contrast, the Tanjungpandan Granite is interpreted as a heat source and heat conductor, contributing to elevated subsurface temperatures. Based on these modeling results, the subsurface structure beneath the Buding hot spring area is dominated by granitic intrusions ascending through fracture or fault zones, facilitating heat transfer and supporting the development of the geothermal system in the region [28, 29].

5. Conclusion

This study presents an integrated interpretation of 2D and 3D gravity modeling to characterize the subsurface structure and geothermal system in the Buding area, East Belitung. The 2D gravity models along profiles A–A' and B–B' yielded low misfit errors of 1.089% and 3.615%, respectively, indicating a good

agreement between observed and calculated data. The modeling results reveal that the subsurface is composed of four principal geological units: Alluvial and Coastal Deposits (Qa), Kelapakampit Formation (PCks), Tanjungpandan Granite (Trtg), and Burungmandi Granodiorite (Kbg). The Tanjungpandan Granite, classified as S-type granite with relatively high density (2.68–2.87 g/cm³), is interpreted as the primary heat source due to its deep-rooted intrusive geometry and potential radiogenic heat production. The Burungmandi Granodiorite (I-type granite) further supports the presence of multiple intrusive phases contributing to regional thermal anomalies. The Kelapakampit Formation, characterized by moderate density values (2.32–2.46 g/cm³) and folded sedimentary lithology, is interpreted as the main geothermal reservoir. Structural deformation within this formation likely enhances secondary permeability, enabling meteoric water infiltration and hydrothermal fluid circulation. The 3D inversion modeling down to a depth of approximately 16.5 km confirms the presence of intrusive granitic bodies beneath the study area. High gravity anomalies in the western sector correspond to dense intrusive units, whereas lower anomalies in the central area reflect sedimentary formations acting as reservoir zones. Overall, the Buding geothermal system is interpreted as an intrusion-related, structurally controlled geothermal system rather than a volcanically dominated system. Heat is generated by deep granitic intrusions and transferred upward through fracture-controlled pathways, where it interacts with permeable sedimentary formations before discharging at surface hot springs. These findings provide new insights into the geothermal potential of East Belitung and highlight the importance of integrated gravity modeling for subsurface characterization in non-volcanic geothermal systems.

CRediT authorship contribution statement

Rabin Fatmansyah: Writing – review & editing, Writing – original draft, Supervision, Software, Resources, Methodology, Investigation, Formal analysis, Data curation. **Rofiqul Umam:** Writing – review & editing, Supervision, Resources, Methodology, Investigation, Formal analysis, Data curation, Conceptualization.

Declaration of Competing Interest

The authors declare that they have no known competing financial interests or personal relationships that could have appeared to influence the work reported in this paper.

Data availability

Data will be made available on request.

Acknowledgment

The authors would like to express their sincere gratitude to all parties who supported this research. We acknowledge the assistance of the local authorities in East Belitung for facilitating field data acquisition in the Buding area. We are also grateful to the technical team for their support during gravity data collection and processing. Special thanks are extended to colleagues and reviewers who provided valuable comments and constructive suggestions that significantly improved the quality of this manuscript.

References

1. Hosono, T., Hartmann, J., Louvat, P., Amann, T., Washington, K. E., West, A. J., Okamura, K., Böttcher, M. E., and Gaillardet, J. (2018). Earthquake-Induced Structural Deformations Enhance Long-Term Solute Fluxes from Active Volcanic Systems, *Scientific Reports*, Vol. 8, No. 1, 1–12. doi:10.1038/s41598-018-32735-1.
2. Zhang, Z., Yao, H., Wang, W., and Liu, C. (2021). 3-D Crustal Azimuthal Anisotropy Reveals Multi-Stage Deformation Processes of the Sichuan Basin and Its Adjacent Journal of Geophysical Research : Solid Earth, *Journal of Geophysical Research: Solid Earth*, Vol. 127, No. e2021JB023289, 1–17. doi:10.1029/2021JB023289.
3. Liu, S., Suardi, I., Xu, X., Yang, S., and Tong, P. (2021). The Geometry of the Subducted Slab Beneath Sumatra Revealed by Regional and Teleseismic Traveltime Tomography, *Journal of Geophysical Research: Solid Earth*, Vol. 126, No. 1, 1–29. doi:10.1029/2020JB020169.
4. Dewi, K. C. S., Siregar, R. N., Ningati, T. I., Pulungan, Z. N., Indriyawati, A., and Takahashi, H. (2025). Analysis of Subsurface Faults Using 3D Gravity Method Based On Satellite Image Data : Insights into Indo-Australian and Eurasian Plate Subduction in the Formation of An Accretionary Prism, *International Journal of Hydrological and Environmental for Sustainability*, Vol. 4, No. 3, 135–148.
5. Hariyono, E., and S, L. (2018). The Characteristics of Volcanic Eruption in Indonesia, *Volcanoes - Geological and Geophysical Setting, Theoretical Aspects and Numerical Modeling, Applications to Industry and Their Impact on the Human Health*, No. July. doi:10.5772/intechopen.71449.
6. McCaffrey, R. (2009). The Tectonic Framework of the Sumatran Subduction Zone, *Annual Review of Earth and Planetary Sciences*, Vol. 37, 345–366. doi:10.1146/annurev.earth.031208.100212.
7. Hristov, V., Stoyanov, N., Valtchev, S., Kolev, S., and Benderev, A. (2019). Utilization of Low Enthalpy Geothermal Energy in Bulgaria, *IOP Conference Series: Earth and Environmental Science*, Vol. 249, No. 1. doi:10.1088/1755-1315/249/1/012035.
8. Taruna, R. M., and Banyunegoro, V. H. (2018). Earthquake Relocation Using Double Difference Method for 2D Modelling of Subducting Slab and Back Arc Thrust in West Nusa Tenggara, *Jurnal Penelitian Fisika Dan Aplikasinya (JPFA)*, Vol. 8, No. 2, 132. doi:10.26740/jpfa.v8n2.p132-143.
9. Collings, R., Lange, D., Rietbrock, A., Tilmann, F., Natawidjaja, D., Suwargadi, B., Miller, M., and Saul, J. (2012). Structure and Seismogenic Properties of the Mentawai Segment of the Sumatra Subduction Zone Revealed by Local Earthquake Traveltime Tomography, *Journal of Geophysical Research*, Vol. 117, 1–23. doi:10.1029/2011JB008469.
10. Jihad, A., Muksin, U., Syamsidik, and Ramli, M. (2021). Earthquake Relocation to Understand the Megathrust Segments along the Sumatran Subduction Zone, *IOP Conference Series: Earth and Environmental Science*, Vol. 630, 012002. doi:10.1088/1755-1315/630/1/012002.
11. Xu, J., and Kono, Y. (2002). Geometry of Slab, Intraslab Stress Field and Its Tectonic Implication in the Nankai Trough, Japan, *Earth, Planets and Space*, Vol. 54, No. 7, 733–742. doi:10.1186/BF03351726.
12. Kusuhara, F., Kazahaya, K., Morikawa, N., Yasuhara, M., Tanaka, H., Takahashi, M., and Tosaki, Y. (2020). Original Composition and Formation Process of Slab-Derived Deep Brine from Kashio Mineral Spring in Central Japan, *Earth, Planets and Space*, Vol. 72, No. 1. doi:10.1186/s40623-020-01225-y.
13. Malod, J. A., Karta, K., Beslier, M. O., and Zen, M. T. (1995). From Normal to Oblique Subduction: Tectonic Relationships between Java and Sumatra, *Journal of Southeast Asian Earth Sciences*, Vol. 12, Nos. 1–2, 85–93. doi:10.1016/0743-9547(95)00023-2.
14. Li, C. F. (2011). An Integrated Geodynamic Model of the Nankai Subduction Zone and Neighboring Regions from Geophysical Inversion and Modeling, *Journal of Geodynamics*, Vol. 51, No. 1, 64–80. doi:10.1016/j.jog.2010.08.003.
15. Stern, R. J. (2002). Subduction Zones, *Reviews of Geophysics*, Vol. 40, No. 4, 3-1-3–38. doi:10.1029/2001RG000108.
16. Utama, H. W., Mulyasari, R., and Said, Y. M. (2021). Geothermal Potential on Sumatra Fault System To Sustainable Geotourism in West Sumatra, *JGE (Jurnal Geofisika Eksplorasi)*, Vol. 7, No. 2, 126–137. doi:10.23960/jge.v7i2.128.
17. Tabei, T., Hashimoto, M., Miyazaki, S., Hirahara, K., Kimata, F., Matsushima, T., Tanaka, T., Eguchi, Y., Takaya, T., Hoso, Y., Ohya, F., and Kato, T. (2002). Subsurface Structure and Faulting of the Median Tectonic Line, Southwest Japan Inferred from GPS Velocity Field, *Earth, Planets and Space*, Vol. 54, No. 11, 1065–1070. doi:10.1186/BF03353303.
18. Tongkul, F. (2017). Active Tectonics in Sabah – Seismicity and Active Faults, *Bulletin of the Geological Society of Malaysia*, Vol. 64, No. December, 27–36. doi:10.7186/bgsm64201703.
19. Maryanto, S. (2017). Geo Techno Park Potential at Arjuno-Welirang Volcano Hosted Geothermal Area, Batu, East Java, Indonesia (Multi Geophysical Approach), *AIP Conference Proceedings*, Vol. 1908, No. 2017. doi:10.1063/1.5012712.
20. Sujitapan, C., Kendall, J. M., Chambers, J. E., and Yordkayhun, S. (2024). Landslide Assessment through Integrated Geoelectrical and Seismic Methods: A Case Study in Thungsong Site, Southern Thailand, *Heliyon*, Vol. 10, No. 2. doi:10.1016/j.heliyon.2024.e24660.

21. Chambers, J., Holmes, J., Whiteley, J., Boyd, J., Meldrum, P., Wilkinson, P., Kuras, O., Swift, R., Harrison, H., Glendinning, S., Stirling, R., Huntley, D., Slater, N., and Donohue, S. (2022). Long-Term Geoelectrical Monitoring of Landslides in Natural and Engineered Slopes, *Leading Edge*, Vol. 41, No. 11, 768–767. doi:10.1190/tle41110768.1.

22. Whiteley, J. S., Watlet, A., Uhlemann, S., Wilkinson, P., Boyd, J. P., Jordan, C., Kendall, J. M., and Chambers, J. E. (2021). Rapid Characterisation of Landslide Heterogeneity Using Unsupervised Classification of Electrical Resistivity and Seismic Refraction Surveys, *Engineering Geology*, Vol. 290, No. May, 106189. doi:10.1016/j.enggeo.2021.106189.

23. Martinho, E. (2023). *Electrical Resistivity and Induced Polarization Methods for Environmental Investigations: An Overview*, *Water, Air, and Soil Pollution* (Vol. 234), Springer International Publishing. doi:10.1007/s11270-023-06214-x.

24. Kusumayudha, S. B., Lestari, P., and Paripurno, E. T. (2018). Eruption Characteristic of the Sleeping Volcano, Sinabung, North Sumatera, Indonesia, and SMS Gateway for Disaster Early Warning System, *Indonesian Journal of Geography*, Vol. 50, No. 1, 70–77. doi:10.22146/ijg.17574.

25. Meju, M. A., and Le, L. (2002). Geoelectromagneticexploration For Natural Resources:Models, Case Studies and Challenges, *Surveys in Geophysics*, Vol. 23, 133–205.

26. Lange, D., Tilmann, F., Henstock, T., Rietbrock, A., Natawidjaja, D., and Kopp, H. (2018). Structure of the Central Sumatran Subduction Zone Revealed by Local Earthquake Travel-Time Tomography Using an Amphibious Network, *Solid Earth*, Vol. 9, No. 4, 1035–1049. doi:10.5194/se-9-1035-2018.

27. Lin, J. Y., Sibuet, J. C., Hsu, S. K., and Wu, W. N. (2014). Could a Sumatra-like Megathrust Earthquake Occur in the South Ryukyu Subduction Zone?, *Earth, Planets and Space*, Vol. 66, No. 1, 1–8. doi:10.1186/1880-5981-66-49.

28. Siringoringo, L. P., Sapiie, B., Rudyawan, A., and Sucipta, I. G. B. E. (2024). Origin of High Heat Flow in the Back-Arc Basins of Sumatra: An Opportunity for Geothermal Energy Development, *Energy Geoscience*, Vol. 5, No. 3, 100289. doi:10.1016/j.engeos.2024.100289.

29. Hochstein, M. P., and Sudarman, S. (1993). Geothermal Resources of Sumatra, *Geothermics*, Vol. 22, No. 3, 181–200. doi:10.1016/0375-6505(93)90042-L.